**Summary:** The effect of electron-beam (EB) irradiation on interfacial adhesion in bioflour (rice-husk flour, RHF)-filled poly(propylene) (PP) biocomposites in which either only the RHF had been EB irradiated or the whole biocomposite had been EB irradiated was examined at different EB-irradiation doses. The tensile strengths of PP–RHF biocomposites with EB-irradiated RHF and EB-irradiated PP and PP–RHF biocomposites were slightly higher than those of the non-irradiated samples. The improved interfacial adhesion of PP–RHF biocomposites with EB radiated RHF and the EB-irradiated PP–RHF biocomposites compared with the non-irradiated samples was confirmed by the morphological characteristics. In addition, the thermal stability of EB-treated biocomposites was slightly higher than those of nonirradiated samples at the irradiation doses of 2 and 5 Mrad. However, at the high irradiation dose (30 Mrad), the tensile strengths of the biocomposites were slightly decreased by main-chain scission (degradation) of PP and RHF. Attenuated total reflectance FT-IR and X-ray-photoelectron-spectroscopy findings confirmed this result by showing that that EB irradiation changed the functional groups of RHF, PP, and the biocomposites and improved the surface characteristics of the biocomposites. The thermal characteristics of the EB-irradiated PP and biocomposites were investigated using differential scanning calorimetry. From the results, we concluded that use of low-dose EB radiation increases the interfacial adhesion between matrix polymer and biofiller.

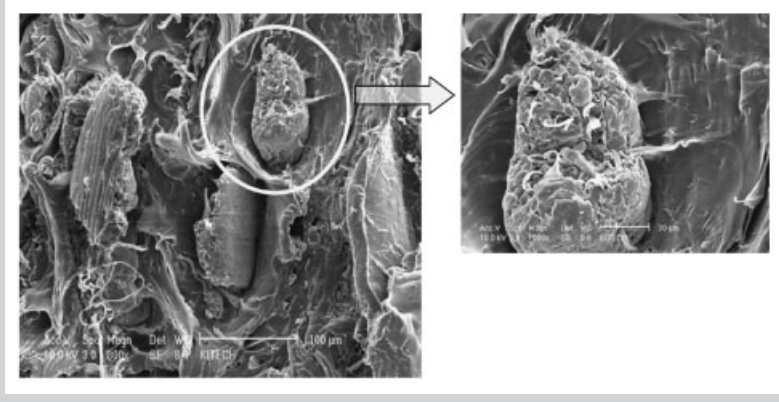

# Enhanced Interfacial Adhesion of Bioflour-Filled Poly(propylene) Biocomposites by Electron-Beam Irradiation

*Hee-Soo Kim, Sumin Kim, Hyun-Joong Kim**

Laboratory of Adhesion & Bio-Composites, Program in Environmental Materials Science, Seoul National University, Seoul 151-921, South Korea
Fax: +82-2-873-231; E-mail: hjokim@snu.ac.kr

Received: March 14, 2006; Revised: April 4, 2006; Accepted: April 24, 2006; DOI: 10.1002/mame.200600121

**Keywords:** biocomposites; bioflour; differential scanning calorimetry (DSC); ecomaterials; interfacial adhesion; electron beam attenuated total reflectance FT-IR; irradiation; X-Ray Photoelectron Spectroscopy

## Introduction

Ecofriendly biocomposites have been used as biofibers and flour for reinforcement to reduce global petroleum dependency, environment problems, and the total mass of final product because of the low density of these biofillers. These biofillers have several advantages over inorganic fillers as reinforcements as a result of their light weight, renewability, low cost, reduced abrasion during production process, ecofriendliness, and biodegradability.[1,2] However, main disadvantage of using these biofillers as the reinforcing filler in biocomposites is the reduced physical,

mechanical, and thermal properties as the biofiller content increases.[2,3] This is a result of weak interfacial adhesion between the hydrophilic biofillers and the hydrophobic polymer matrix. Biofillers mainly contain hydroxyl groups of cellulose and hemicellulose molecules which reduce the bonding and wetting of biocomposites because of poor compatibility with hydrophobic matrix (polyolefin).[3,4] Therefore, various methods studied in recent years to improve the interfacial adhesion between the biofillers and the matrix polymer by modifying the biofiller surface have included the use of maleic-anhydride-grafted poly(propylene) (PP-*g*-MA),[5] the addition of silane coupling agents,[6] surface chemical modification,[7] and plasma treatment[8] of the biofiller. Pretreatment of the matrix polymer and chemically modified biofillers offer good physical, mechanical, and thermal properties and interfacial bonding of biocomposites at the interface.

In the present study we deal with the effects of electron beam (EB) irradiation on bioflour and biocomposites to improve interfacial adhesion and we investigate the influence of this treatment on the mechanical and thermal properties of the biocomposites. Electron accelerators are widely used in printing companies, tire companies, the automobile industry, and cable factories for curing and cross-linking of polymeric materials.[9–11] The EB-irradiation method has been known to change the physical properties of polymers by macromolecule cross-linking (curing) and main-chain scission (degraded) in high radiation energy and graft polymerization.[12] The advantages of processing with electron accelerators are short processing time, that it is a unique process, a noncatalytic and environmentally friendly process, and is easily automated.[13] In addition, as a new method for the modification of biofiller surface, the EB process does not use maleic anhydride-grafted copolymers (compatibilizing agents) and chemical modifiers. Therefore, we can use it as a radiation method for surface modification of bioflour to enhance the interfacial interaction of biocomposites.

The use of rice-husk flour (RHF) as a biofiller in a poly(propylene) (PP) matrix offers environmental benefits and an economical solution for the increasing costs of wood-based materials and construction materials for applications such as decking, siding, roofing, window frames, and automotive interior parts.[14,15] This is because of the improved properties of biocomposite materials, such as better dimensional stability, in comparison with wood-based materials.

In this study we aim to investigate the influence on the interfacial adhesion of different doses of EB irradiation biocomposites of on PP–RHF biocomposites in which either only the RHF has been EB irradiated (30 wt.-% filler loading) or the whole composite has been EB irradiated. We compared the mechanical and thermal properties, chemical structure, surface characterization, and morphological behavior of EB-irradiated and nonirradiated biocomposites. The results support our recommendation of the EB process as an environmentally friendly, new method to enhance interfacial bonding in bioflour-polymer composites.

## Experimental Part

### *Materials*

RHF, used as the biofiller, was supplied by Saron Filler Co., South Korea. The mean particle diameter was 300 μm. The chemical constituents of RHF are shown in Table 1. PP in the form of homopolymer pellets, used as the matrix polymer, was supplied by GS Caltex Corp., South Korea. PP had a density of $0.91 g \cdot cm^{-3}$ and a melt flow index of $1.2 g \cdot min^{-1}$ (230 °C/2,160g).

### *EB-Irradiated Bioflour and Biocomposites*

RHF was irradiated with EB at radiation doses of 1, 2, 5, 10, 30, and 50 Mrad using an EB accelerator at EB-TECH Co., South Korea. The prepared PP (pellets and tensile specimens) and biocomposites at 30 wt.-% filler loading (pellets and tensile specimens) were also irradiated with EB at radiation doses of 1, 2, 5, 10, and 30 Mrad. The irradiation was performed at room temperature (25 °C) and room humidity, and in the presence of oxygen. EB had an energy output of 1 MeV, beam current of 1mA, and velocity of $10 m \cdot min^{-1}$. Figure 1 presents a schematic diagram of the EB-treatment equipment.

### *Compounding and Sample Preparation*

RHF was oven dried at 105 °C for 24 h to reduce the moisture content to ≈1%–3% and then stored in sealed polyethylene bags before compounding. The matrix polymers, PP, were blended with the RHF in a laboratory-sized, corotating, twin-screw extruder using three general processes: melt blending, extrusion, and pelletizing. The extruder barrel was divided into eight zones with the temperature in each zone being individually adjustable. The temperature mixing zone of the barrel was maintained at 190 °C with a screw speed of 250 rpm. The extruded strand was cooled in a water bath and pelletized using a pelletizer. Extruded pellets were dried at 80 °C for 24 h and stored in sealed polyethylene bags to avoid moisture infiltration. To investigate the effect of composition on the tensile strength of the biocomposites, four levels of filler loadings were prepared: 10, 20, 30 and 40 wt.-%. Also examined was the effect of adding EB-irradiated RHF at 30 wt.-% filler loading on the interfacial adhesion of the biocomposites.

Table 1. Chemical constituents of RHF.

| | Holocellulose | Lignin | Ash | Others | Total |
|---|---|---|---|---|---|
| | % | % | % | % | % |
| Rice-husk flour[a)] | 60.8 | 21.6 | 12.6 | 5.0 | 100 |
| Rice-husk flour[b)] | 59.9 | 20.6 | 13.2 | 6.3 | 100 |

[a)] Rice-husk and wood flours from ref.[2]
[b)] Specification from Saron Filler Co.

 

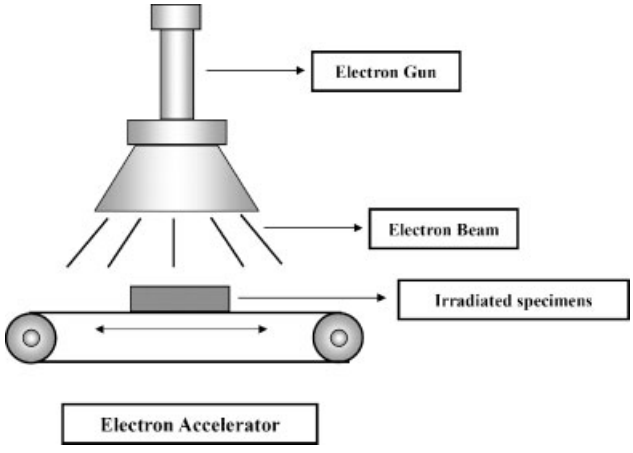


Figure 1. Schematic diagram of the EB-irradiation equipment.

Tensile-strength (ASTM D 638) test specimens were injection molded using an injection molding machine (Bau Technology, South Korea) at 190 °C with an injection pressure of 1 200 psi. After molding, the specimens were conditioned before testing at 50 ± 5% of rice husk for at least 40 h according to ASTM D 618-99.

*Tensile Strength*

The tensile tests were conducted according to ASTM D 638-99 with a Universal Testing Machine (Zwick Co.) at a crosshead speed of 100 mm · min$^{-1}$ and a room temperature of 20 ± 2 °C. Five measurements were conducted and each value obtained was determined from the average of five samples.

*Thermal Properties*

Thermogravimetric Analysis (TGA)

TGA measurements of the PP–RHF biocomposites with EB-irradiated RHF and EB-irradiated PP–RHF biocomposites were carried out using a thermogravimetric analyzer (TA instruments, TGA Q500) on samples of about ≈10–13 mg, over a temperature range from 25 °C to 700 °C, at a heating rate of 20 °C · min$^{-1}$, under a nitrogen flow of 0.040 l · min$^{-1}$. TGA was measured with the biocomposites placed in a high-quality nitrogen (99.5% nitrogen, 0.5% oxygen content) atmosphere to prevent unwanted oxidation.

Differential Scanning Calorimetry (DSC) Analysis

DSC analysis was carried out using a TA Instrument DSC Q 1000 (NICEM at Seoul National University) with ≈3–5 mg of the PP–RHF biocomposites with EB-irradiated RHFand EB-irradiated PP and PP–RHF biocomposites at the designated time points. Each sample was scanned as the dynamic mode was raised from −80 to 200 °C at a heating rate of 10 °C · min$^{-1}$ and then cooled at the same rate under a nitrogen atmosphere. Glass transition ($T_g$), melting ($T_m$), and crystallization ($T_c$) temperatures were determined from the second scan. $T_m$ was taken as the maximum of the endothermic melting peak, $T_c$ as the temperature at the top of the crystallization peak, and $T_g$ as the deflection of the baseline from the cooling scan. The heats of fusion ($\Delta H_f$) and crystallization ($\Delta H_c$) were determined from the areas of the melting and crystallization peaks, respectively.

In order to measure the relative degree of crystallinity ($X$) of EB-irradiated and nonirradiated specimens, the follow equation was used:

$$X = \frac{\Delta H}{\Delta H_{100}} 100$$

where $\Delta H$ is the heat of crystallization of the PP and biocomposites and $\Delta H_{100}$ is the value of heat of crystallization for 100% crystalline PP ($\Delta H_{100} = 209$ J · g$^{-1}$).[16]

*FT-IR Measurements*

FTIR spectra of EB-irradiated RHF were obtained using a Thermo Nicolet Nexus 870 FT-IR spectrophotometer from the U.S.A. Irradiated RHF (2 mg) was ground with KBr pellets (10 mg) and then dispersed to obtain the followed by compression at 167 MPa to form sheets. The infrared spectra in the attenuated total reflectance (ATR) FT-IR spectra of the PP–RHF biocomposites with EB-irradiated RHF, EB-irradiated PP, and EB-irradiated biocomposites were obtained using a Thermo Nicolet Nexus 870 FTIR spectrophotometer from the United States. A diamond was used as an ATR crystal. The specimens were analyzed over the range of 525–4 000 cm$^{-1}$ with a spectrum resolution of 4 cm$^{-1}$. All spectra were averaged over 32 scans. This analysis was performed at point-to-point contact with a pressure device when analyzing the biocomposites.

*X-Ray Photoelectron Spectroscopy (XPS)*

X-ray photoelectron spectra of EB-irradiated biocomposites were obtained with a Sigma Probe (Thermo VG, UK) analyzer. The spectra were recorded using a monochromatic Al-$K_\alpha$ radiation X-ray source, with 50 W operating at 10 kV voltage, and base pressure of $4 \times 10^{-8}$ Torr in the sample chamber. XPS spectra were collected in the range of 0–1 200 eV binding with a resolution of 1.0 eVand a pass energy of 50 eV. The XPS spectra were analyzed using a commercial, curve-fitting software.

*Morphological Test*

Scanning electron microscopy was used to measure the fracture surfaces of the EB-irradiated and nonirradiated tensile specimens using a SIRIOM scanning electron microscope (SEM) (FEI Co.) from the United States. Prior to the measurement, the specimens were coated with gold (purity, 99.99%) to eliminate electron charging.

## Results and Discussion

### *Tensile Strength*

Figure 2 shows the tensile strength of PP–RHF biocomposites at different RHF loadings. The tensile strength of the biocomposites decreased with increasing filler loading.

 

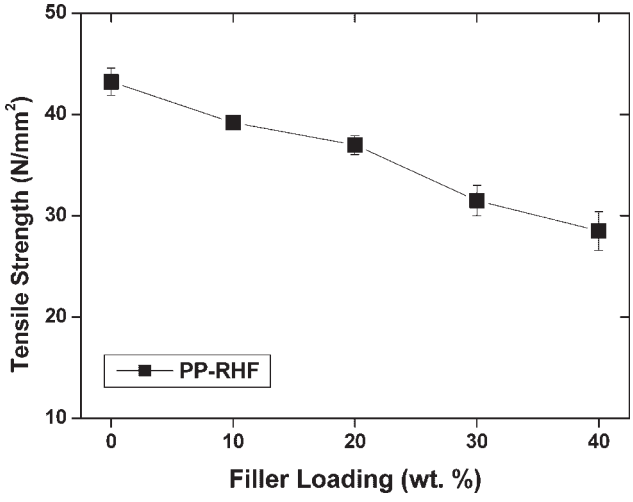


Figure 2. Tensile strength of RHF-filled PP biocomposites.

RHF contains the hydroxyl groups of cellulose and hemicellulose ingredients which reduce the interfacial adhesion and wetting between the RHF (hydrophilic) and PP (hydrophobic).[3,17] This explains why the commercial application of biocomposites has been restricted by the low mechanical properties of biocomposites with high content of bioflour – because of low compatibility at the interface. The tensile strengths of PP–RHF biocomposites with nonirradiated RHF and with RHF EB irradiated at different doses are shown in Figure 3. The pretreatment of hydroxyl groups on RHF can be achieved with EB radiation and can work effectively to increase interfacial adhesion between the RHF molecules and the PP matrix. The tensile strength of biocomposites with EB-irradiated RHF at low radiation doses (1, 2, 5 and 10 Mrad) was higher than those with nonirradiated RHF. This is due to the reduction of hydrophilic OH groups from RHF and the removal of impurities by the emission of active hydroxyl and free radicals as a result of the RHF surface being EB irradiated.[14] The reduction of OH groups and impurities from RHF can lead to improved interaction between the RHF surface and PP matrix. An EB radiation dose of 2 Mrad on RHF gave the highest tensile strength and was therefore chosen as the proper radiation dose to improve interfacial adhesion. In contrast, the tensile strength of the biocomposites decreased slightly with increasing radiation dose, up to 30 Mrad, possibly because the main chain of RHF was degraded at a high radiation dose (50 Mrad) conditions.

The tensile strengths of the EB-irradiated biocomposites at 30 wt.-% filler loading and EB-irradiated PP with irradiation doses of 1, 2, 5, 10 and 30 Mrad are shown in Figure 4(a) and 4(b). The tensile strengths of EB-irradiated PP and biocomposites are clearly higher than those of

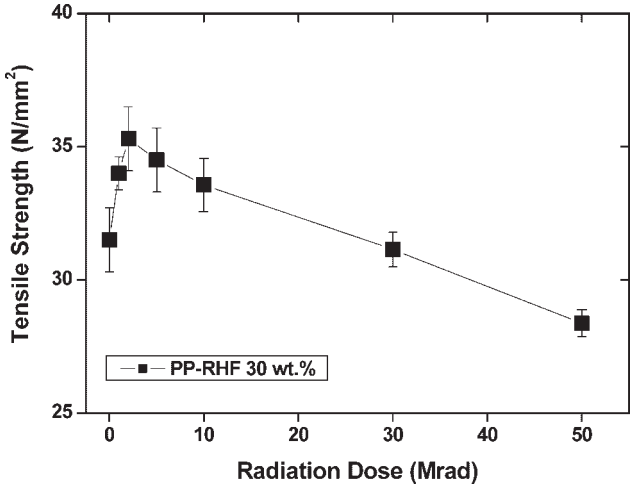


Figure 3. Tensile strength of PP–RHF biocomposites with RHF EB irradiated at different irradiation doses.

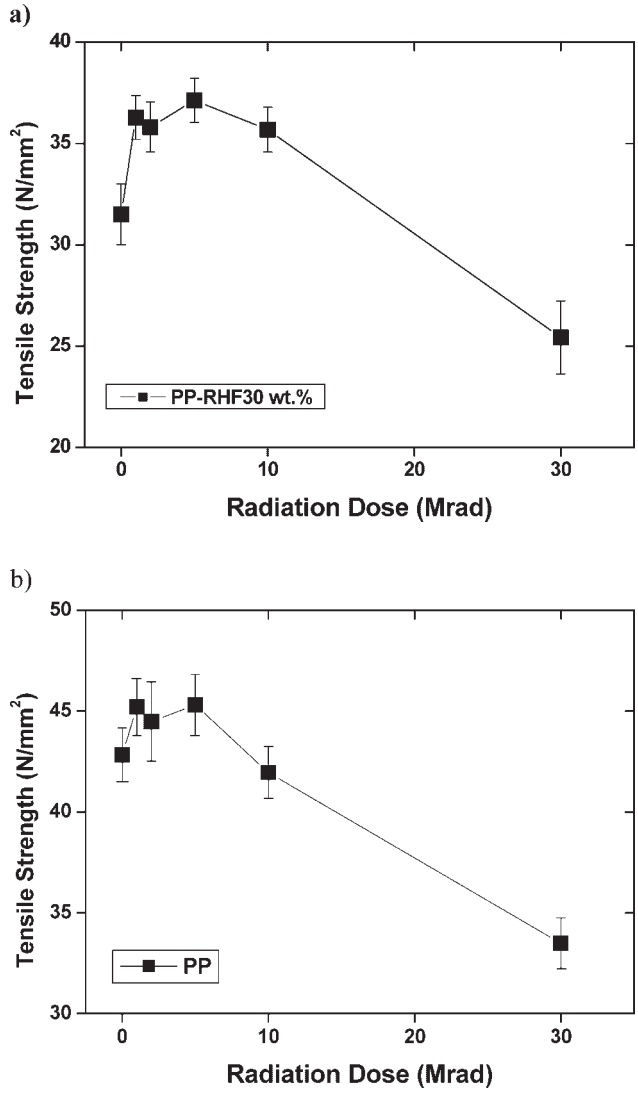


Figure 4. Tensile strength of (a) biocomposites, and (b) PP EB irradiated at different irradiation doses.

 

nonirradiated PP at irradiation doses of 1, 2, 5, and 10 Mrad. However, as irradiation dose increased to 30 Mrad, the tensile strengths of PP and biocomposites decreased remarkably. The increase of the tensile strength was due to the slightly increased cross-linking in the amorphous region of PP and the better interaction between RHF and PP.[8,14,18] Khan et al.[19] reported that the tensile strength of EB-irradiated biodegradable polybutylene succinate (PBS) at low irradiation dose was slightly increased as a result of the formation of additional cross-linking in PBS from the production of mainly polymer radicals and hydrogen radicals. The decreased tensile strengths of PP and biocomposites at 30 Mrad dose have resulted from the structural distortion and random chain scission of the PP main chain through the formation of peroxy and hydroperoxy radicals with the high EB radiation energy.[16,18,19] Therefore, this result shows that the EB irradiation method not only increased the strength of the matrix polymer, but also improved the interaction between the bioflour and matrix polymer at low irradiation dose.

### *Morphological Characteristics*

Figure 5(a) and (b) shows the SEM micrograph taken from the tensile-fracture surface of PP with nonirradiated RHF at 30 wt.-% filler loading. Figure 5(a) shows many RHFs had been removed completely from the matrix in the tensile fracture surface. The weak interface between the RHF and PP can be clearly observed in Figure 5(b). This weak interface is a result of the poor and weak interaction between the RHF and the matrix polymer. The poor interaction can be explained by the low compatibility between the polar functional groups of RHF and nonpolar PP.[3,4] The tensile-fracture surface of PP biocomposites filled with RHF (30 wt.-%) which had been irradiated at 2 Mrad is shown in Figure 6(a). There is little evidence in the SEM micrographs of samples which had undergone the EB-treatment process that RHF particles have been removed from the PP matrix. This result is also evident in the tensile-fracture micrograph of EB-irradiated biocomposites at the irradiation dose of 5 Mrad, shown in Figure 7(a). The strong interface can clearly be observed in Figure 6(b) and 7(b). This indicates that in the PP–RHF biocomposites with EB-irradiated RHF and in the EB-irradiated PP–RHF biocomposites there was better dispersion and interfacial adhesion.[3,20] This result is thought to have enhanced the mechanical properties of the biocomposite materials.

### *Thermogravimetric Analysis*

The TGA curves for PP–RHF biocomposites with EB-irradiated RHF (30 wt.-%) and EB-irradiated biocomposites are presented in Figure 8 and 9, respectively. In the all TGA curves, two thermal-degradation regions can be observed: the first is due to thermal depolymerization of cellulose, hemicellulose, and lignin in RHF[1,2], and the second is due to random chain scission of the PP main chains.[21] This result indicates that the thermal stability and decomposition temperature of PP were higher than those of RHF. The thermal stability and decomposition temperature of PP–RHF biocomposites with EB-irradiated RHF and EB-irradiated PP–RHF biocomposites were slightly higher than those of nonirradiated samples at the irradiation doses of 2 and 5 Mrad. However, compared with nonirradiated RHF-filled PP biocomposites, there was no difference in the thermal stability of the PP–RHF biocomposites with RHF EB irradiated at 10, 30, and 50 Mrad. The improved thermal stability of EB-irradiated biocomposites was attributed to the fact that a strong interaction between RHF and PP was induced by EB radiation.[18,19] However, in the case of the 30 Mrad dose (Figure 9), the thermal stability of the biocomposites was slightly lower than samples with lower

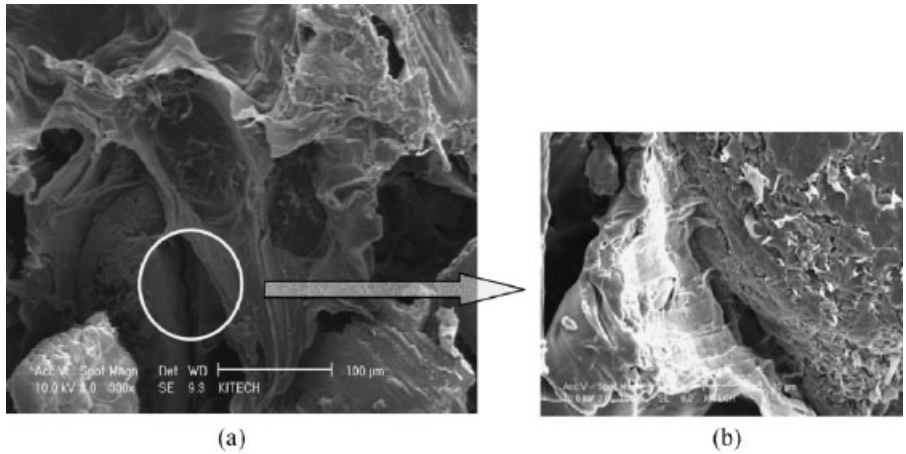


(a) (b)

Figure 5. SEM micrographs of nonirradiated PP–RHF biocomposites at magnifications of (a) 300× and (b) 1 000×.

 

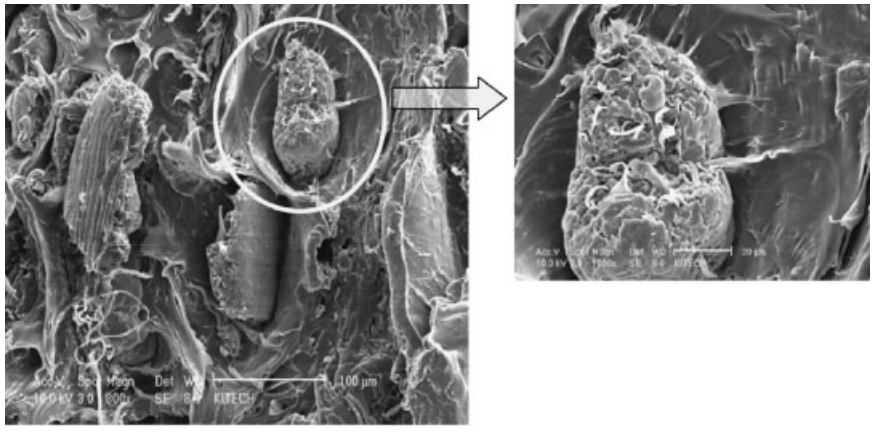

(a) (b)

Figure 6. SEM micrographs of PP–RHF biocomposites with RHF EB irradiated at 2 Mrad at magnifications of (a) 300× and (b) 1 000×.

irradiation doses at low temperatures (between 250 to 350 °C) because the high-energy irradiation contributed to chain cleavage (degradation) in the biocomposites.[9,12] This result supported the remarkably decreased tensile strength of EB-irradiated biocomposites at the irradiation dose of 30 Mrad.

### *DSC Analysis*

Figure 10(a) and 10(b) presents the second-cooling thermograms and the second-heating thermograms, respectively, for PP–RHF biocomposites with RHF EB irradiated at different irradiation doses. The $T_g$, $T_m$, and $T_c$ of biocomposites were not significantly affected by the addition of EB-irradiated RHF. However, Table 2 shows that $\Delta H_f$, $\Delta H_c$, and the degree of crystallinity of PP–RHF biocomposites with EB-irradiated RHF were slightly increased by irradiation doses of 2 Mrad and 5 Mrad. This is attributed to the strong interfacial interaction between PP and RHF as a result of the RHF being EB irradiated. Joseph et al.[21] reported that the crystallinity and $\Delta H_c$ of PP–sisal-fibre composites, which had undergone surface modification by chemical treatments and the addition of maleic anhydride modified PP (MAPP), were higher than those of nontreated samples as a result of the favorable interaction between the sisal fibers and PP. The $\Delta H_f$ and $\Delta H_c$ of the polymer materials revealed the degree of crystallinity in the molecular structure, because higher $\Delta H_f$ and $\Delta H_c$ values correspond to a higher degree of crystallinity.[9] These results were also seen in the EB-irradiated biocomposites and PP. This behavior may have been caused by the additional cross-linking in amorphous and crystalline regions of PP and by the enhanced interfacial adhesion of the biocomposites.[14,18,19] However, at the high irradiation dose of 30 Mrad, $T_m$, $\Delta H_f$, $\Delta H_c$, and the degree of crystallinity of EB-irradiated PP and biocomposites all decreased

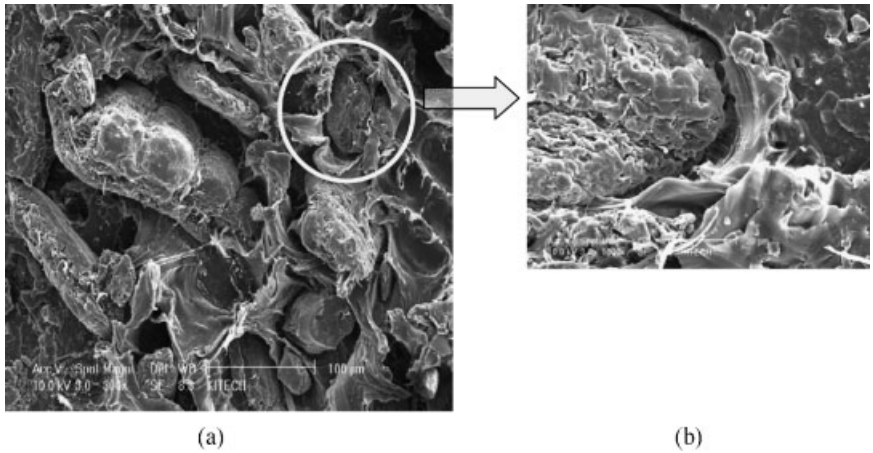

(a) (b)

Figure 7. SEM micrographs of EB -irradiated (5 Mrad) PP–RHF biocomposites at magnifications of (a) 300× and (b) 1 000×.

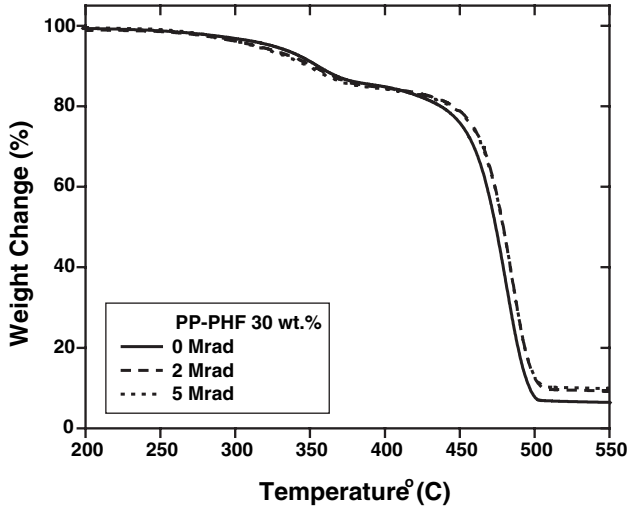


Figure 8. TGA curves of PP–RHF biocomposites with RHF which was nonirradiated and with RHF which was EB irradiated at different irradiation doses.

as a result of the presence of random chain scissions in both the amorphous and crystalline regions of the PP.[22,23]

### *ATR FT-IR Analysis*

FT-IR spectra measured from RHF EB irradiated with different irradiation doses are shown for comparison in Figure 11. The absorption bands in the region ≈3 700–3 100 $cm^{-1}$ are attributed to hydroxyl (OH) groups stretching the vibrations for RHF. With increasing irradiation dose, the absorption intensity of these peaks decreased, indicating that the EB irradiation of RHF caused the reduction of RHF hydroxyl groups as a result of the formation of excited free radicals and hydrogen radicals of water molecules in air by EB irradiation.[24] This EB

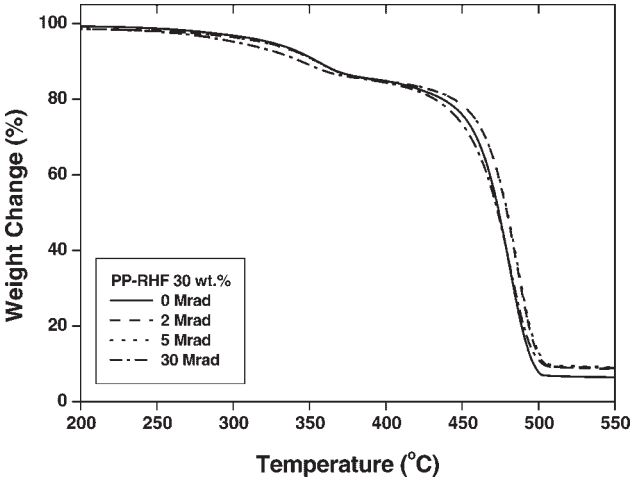


Figure 9. TGA curves of biocomposites which were nonirradiated and EB irradiated at different irradiation doses.

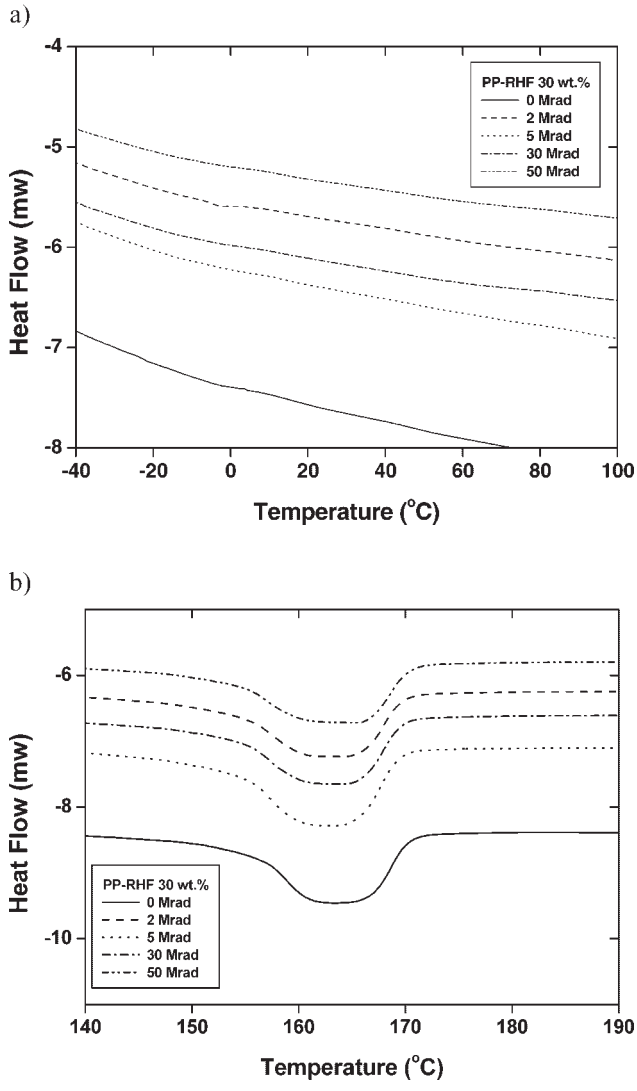


Figure 10. DSC (a) second-cooling thermograms, and (b) second-heating thermograms of PP–RHF biocomposites with RHF EB irradiated at different irradiation doses.

irradiation of RHF contributed to improving the interfacial adhesion due to the reduction in the hydrophilicity and rough surface of the RHF.[8] This result confirmed that the tensile strength of PP biocomposites filled with EB-irradiated RHF (2 and 5 Mrad) was slightly higher than that of the nonirradiated samples.

The same result is seen in the ATR FT-IR spectra of PP biocomposites filled with EB-irradiated RHF at 30 wt.-% filler loading, as shown in Figure 12. The absorbance in the region ≈3 500–3 100 $cm^{-1}$ was mainly due to the O–H stretching vibration and in the range ≈1 650–1 600 $cm^{-1}$ was due to the H–O–H stretching vibration of absorbed water.[25] The intensity of the bending vibration of these peaks decreased with increasing EB-irradiation dose. This is a result of the reduction of the hydroxyl groups of RHF by EB irradiation. The bands at 1 162 $cm^{-1}$ and 1 081 $cm^{-1}$, also seen in Figure 11, were attributed to C–O and C–O–C

 

Table 2. DSC test results of the PP biocomposites filled with EB-irradiated RHF and PP and PP–RHF biocomposites EB irradiated at different irradiation doses.

| Irradiation dose (Mrad) | $T_g$ | $T_m$ | $\Delta H_f$ | $T_c$ | $\Delta H_m$ | Degree of crystallinity |
|---|---|---|---|---|---|---|
| Mrad | °C | °C | $J \cdot g^{-1}$ | °C | $J \cdot g^{-1}$ | % |
| *RHF–PP biocomposites filled with EB-radiated RHF* | | | | | | |
| 0 | −7.4 | 163.5 | 72.1 | 104.8 | 85.9 | 41.1 |
| 2 | −5.5 | 163.4 | 76.5 | 103.2 | 91.2 | 43.6 |
| 5 | −5.1 | 162.9 | 83.6 | 104.2 | 92.3 | 44.1 |
| 30 | −5.3 | 163.8 | 74.3 | 102.2 | 86.5 | 41.4 |
| 50 | −6.4 | 165.4 | 70.1 | 101.2 | 82.9 | 39.7 |
| *EB-irradiated PP–RHF biocomposites* | | | | | | |
| 0 | −7.4 | 163.5 | 72.1 | 104.8 | 85.9 | 41.1 |
| 2 | −8.4 | 164.9 | 82.3 | 107.3 | 92.5 | 44.2 |
| 5 | −9.2 | 163.2 | 87.5 | 105.5 | 97.7 | 46.7 |
| 10 | −9.3 | 163.1 | 88.8 | 104.9 | 95.4 | 45.6 |
| 30 | −10.6 | 154.6 | 82.9 | 103.0 | 86.3 | 41.3 |
| *EB-irradiated PP* | | | | | | |
| 0 | −8.7 | 167.9 | 106.8 | 93.3 | 116.5 | 55.7 |
| 2 | −9.6 | 165.1 | 115.3 | 100.9 | 120.2 | 57.4 |
| 5 | −10.1 | 163.3 | 120.7 | 103.5 | 125.3 | 59.8 |
| 10 | −10.7 | 161.9 | 110.1 | 103.6 | 117.9 | 55.9 |
| 30 | −11.4 | 155.6 | 100.3 | 102.2 | 109.2 | 52.1 |

stretching vibrations of the cellulose and hemicellulose in RHF, respectively. The absorption band in the ≈1 440–1 420 $cm^{-1}$ region was assigned to the C–H aromatic skeletal vibrations of RHF.[18,24] At the high irradiation dose (30 Mrad), the absorption intensity of these peaks was significantly decreased. This was attributed to the chain scission of cellulose, hemicellulose, and lignin by the high-energy EB-irradiation dose. Therefore, we can suggest that high-energy irradiation of RHF is not a suitable surface-treatment method to improve interfacial adhesion between PP and RHF.

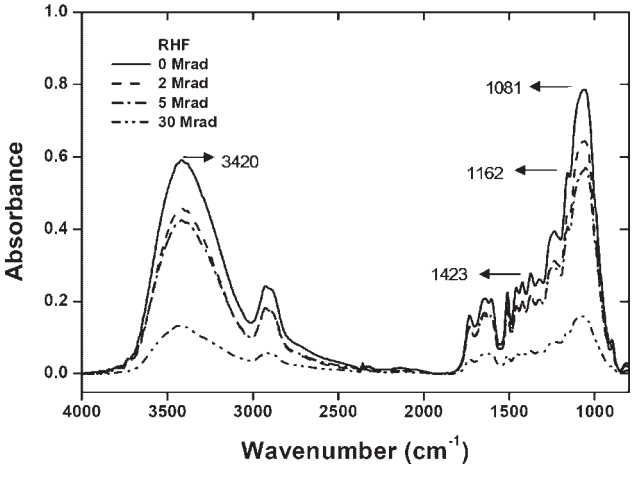


Figure 11. FT-IR spectra of RHF EB irradiated at different irradiation doses.

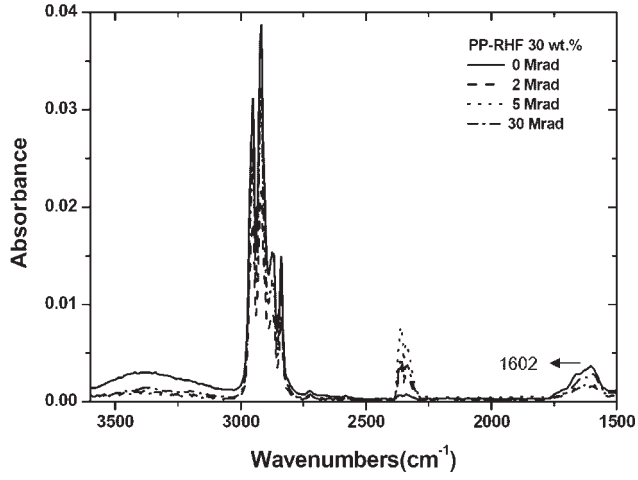


Figure 12. ATR FT-IR spectra of PP biocomposites filled with RHF EB irradiated at different irradiation doses.

Figure 13 presents the ATR FT-IT spectra of PP EB irradiated at different doses. The absorption band at ≈3 500–3 100 $cm^{-1}$ is due to hydroxyl groups of PP. As the EB irradiation dose of PP increased, the intensity of this peak increased slightly. Furthermore, this figure showed new peaks at 1 650 $cm^{-1}$ after the EB irradiation. These peaks were considered to be due to carbonyl group C–O stretching of the irradiation products of PP as a result of surface oxidation of PP, indicating that EB-irradiated PP exhibits higher hydrophilicity than nonirradiated PP. Albano et al.[14] confirmed that the wider band within 3 400–3 300 $cm^{-1}$ on the FT-IR spectrum of gamma-ray-irradiated PP was due to OH stretching. These authors indicated that the oxygen-containing groups, such as carbonyl, carboxylic, and ether, were introduced onto PP chains by gamma-ray radiation. We expected that the increased number of OH radicals of PP may have interacted at the hydrogen bridge between RHF and PP.[14] This result confirms that the tensile strengths of EB-irradiated biocomposites (30 wt.-%) at the irradiation doses of 2 and 5 Mrad were slightly higher than that of the nonirradiated biocomposites. At the low irradiation doses (2 and 5 Mrad), the absorption intensities of C–H (2 883 and 2 836$cm^{-1}$) of PP were slightly decreased, indicating that the cross-linking between the neighboring chains was caused by the formation of hydroxyl, hydroperoxy, and free radicals produced by the cleavage of the C–H bond.[8,26] Also, this figure shows new peaks at 1 740 $cm^{-1}$ for PP after increasing the EB-irradiation dose. These peaks are considered to be due to a carbonyl-group degradation product of PP which was produced by an oxidation reaction associated with the chain scission.[18,26]

However, at the EB irradiation dose of 30 Mrad, the spectra intensities of C–H and $CH_3$ (2 883 and 1 462 $cm^{-1}$, respectively) of PP were significantly decreased. This result, also seen in Figure 14(a), is a consequence of the

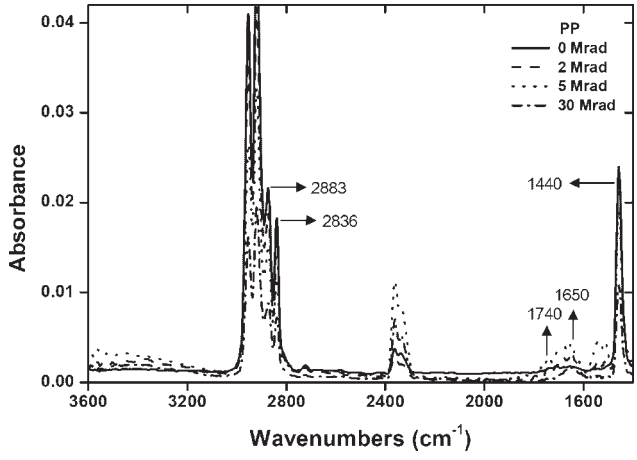


Figure 13. ATR FT-IR spectra of PP EB irradiated at different irradiation doses.

main-chain scission (C–C bond) which occurred mainly in the amorphous PP.[9,18,23] Figure 14(b) shows the absorption peaks at 1 167 and 1 114 $cm^{-1}$, which arose from the C–O stretching vibration of the biocomposites.[25] With increasing EB irradiation, the absorption intensity of these peaks was slightly increased. This result indicated that the additional cross-linking reaction between PP chains and RHF chains was due to the reduction of RHF hydroxyl groups by excited hydrogen and hydroxyl radicals in the EB-irradiation system.[26]

## *XPS Analysis*

Figure 15 shows the XPS spectra of (a) nonirradiated and (b) EB-irradiated (5 Mrad) biocomposites. The EB process in air was conducted by the formation of radicals such as hydrogen, hydroxyl, and free radicals due to oxygen in the air being excited through EB irradiation.[11] The first peaks

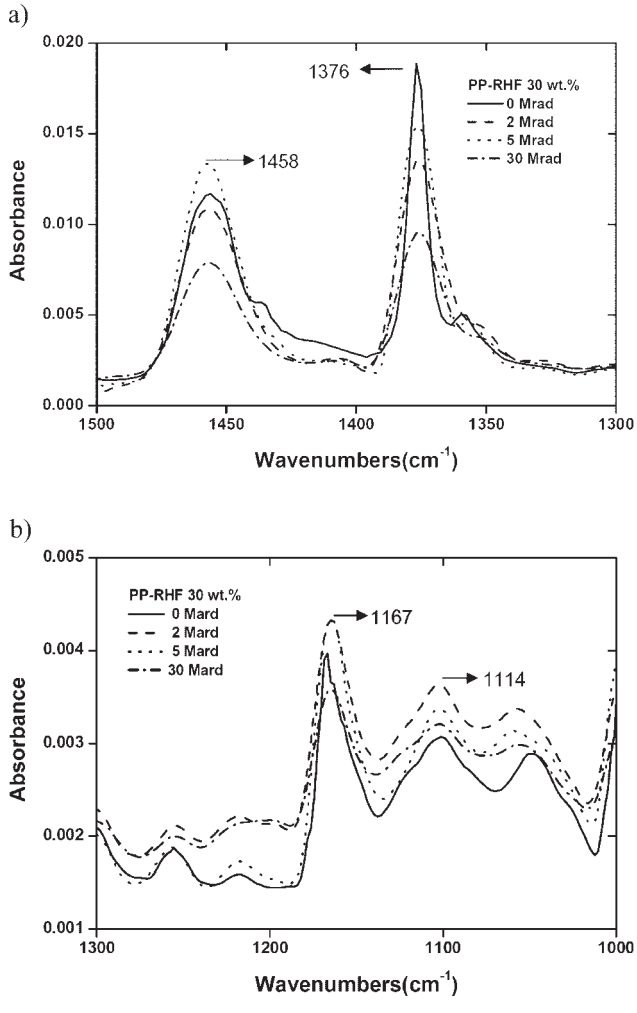


Figure 14. ATR FT-IR spectra of the absorption regions (a) ≈1 500–1 300 $cm^{-1}$, and (b) ≈1 300–1 000 $cm^{-1}$ of biocomposites EB irradiated at different irradiation doses.

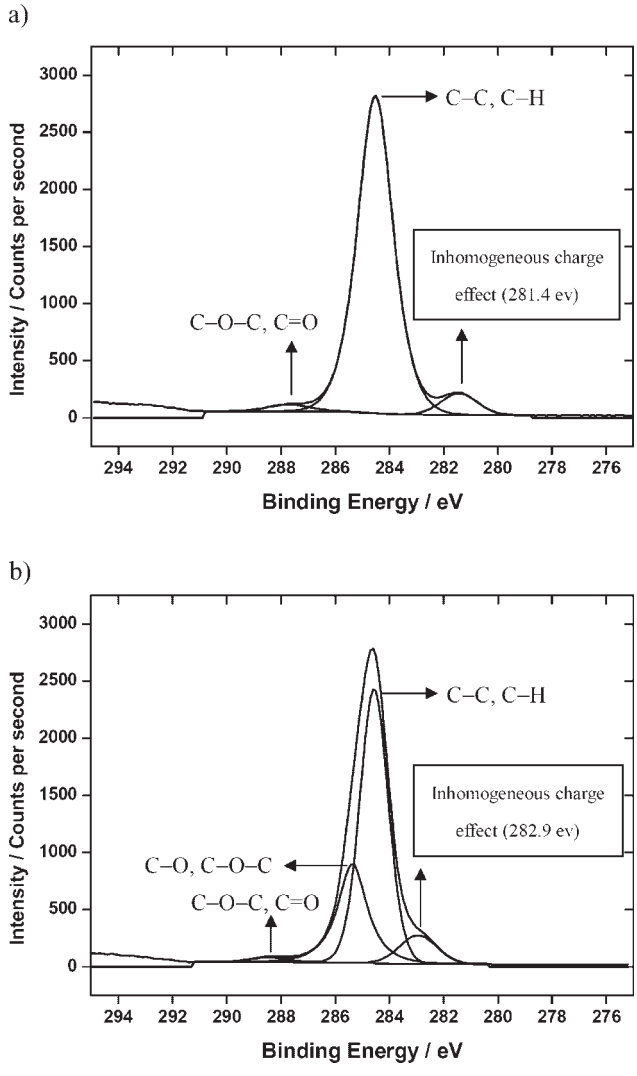


Figure 15. XPS spectra of carbon peaks (C1s) for PP–RHF (a) nonirradiated, and (b) EB irradiated (5 Mrad).

 

Table 3. C1s and O1s peaks in the XPS spectra for EB-irradiated biocomposites.

| PP-RHF 30% | Core level | Corresponding bonds | Peak BE |
|---|---|---|---|
| | | | eV |
| | C1s | C–C, C–H | 284.5 |
| | | C–O–C, C=O | 287.7 |
| | O1s | C=O | 531.8 |
| | | C–OH | 532.3 |
| Biocomposites EB irradiated at 5 Mrad | | | |
| | C1s | C–C, C–H | 284.6 |
| | | C–O, C–O–C | 285.6 |
| | | C–O–C, C=O | 288.5 |
| | O1s | C=O | 531.9 |
| | | C–OH | 532.9 |
| | | O=C–O | 533.7 |
| Biocomposites EB irradiated at 30 Mrad | | | |
| | C1s | C–-C, C–H | 284.6 |
| | | C–O, C–O–C | 285.8 |
| | | C–O–C, C=O | 288.1 |
| | O1s | C=O | 531.8 |
| | | C–OH | 532.8 |
| | | O=C–O | 533.5 |

at (a) 281.4 eV and (b) 282.9 eV can be explained by the inhomogeneous charging on the biocomposite surfaces. As seen in Table 3[8,27,28], EB-irradiated biocomposites exhibited the two new characteristic peaks of C1s (BE = 284.5 eV) and O1s (BE = 533.7 eV). The new characteristic peak of C1s is also seen in Figure 15. The new C1s and O1s peaks were related to C1s (C–O and C–O–C) and O1s (O=C–O) bonding types.[8,27,28] The new C1s (C–O and C–O–C) and O1s (O=C–O) peaks of EB-irradiated biocomposites may have resulted from the removal and oxidation of C–C and C–H structures of biocomposites by excited hydrogen and hydroxyl radicals.[8] The reduction of C–C and C–H structures of the biocomposites clearly indicated that the formation of C–O–C and O=C–O functional groups arose from a slight increase in cross-linking reactions (C–O and C–O–C bonding type) and enhanced interfacial adhesion (esterification reaction: O=C–O bonding type) between RHF and the matrix polymer, compared with the nonirradiation method.[8,18] In addition, we can expect that at the higher EB-irradiation dose (30 Mrad), increased degradation (chain scission) and surface oxidation (C=O, C–O–C, and O=C–O functional groups) will result from the formation of hydroperoxy and hydroperoxide radicals in the amorphous region of the biocomposites. This result was confirmed by the reduction of tensile strength and thermal properties of the biocomposites EB irradiated at 30 Mrad.

## Conclusion

With increased filler loading, the tensile strength of the biocomposites decreased due to the low interfacial adhesion and wetting between RHF (hydrophilic) and PP (hydrophobic). The tensile strength of the biocomposites with EB-irradiated RHF at low radiation doses was higher than that of those with nonirradiated RHF. Also, the tensile strength of EB-irradiated PP and PP–RHF biocomposites followed the same trend as a result of the slight increase in cross-linking in the amorphous region of PP and of the better interaction between RHF and PP. The improved interfacial interaction of PP–RHF biocomposites with EB-treated RHF and EB-treated PP–RHF biocomposites, compared with untreated samples, was confirmed by SEM micrographs showing little evidence RHF particles having been removed from the PP matrix. In addition, the thermal stability of EB-irradiated biocomposites was slightly higher than those of the nonirradiated samples at the irradiation doses of 2 and 5 Mrad. However, with increasing radiation dose up to 30 Mrad, the tensile strength and thermal stability of PP and PP–RHF biocomposites decreased slightly. The $\Delta H_f$, $\Delta H_c$, and crystallinity of EB-irradiated PP and PP–RHF biocomposites were slightly increased at the irradiation doses of 2 and 5 Mrad. In contrast, the $T_m$, $\Delta H_f$, $\Delta H_c$, and crystallinity of EB-irradiated PP and PP–RHF biocomposites decreased at the high irradiation dose of 30 Mrad. These results were confirmed by the changes to the ATR FT-IR spectra of O–H, C–O–C, C–O, C–H, C–C, and $CH_3$ stretching of the functional groups of RHF, PP, and the PP–RHF biocomposites that were observed after EB irradiation. The XPS spectra of EB-irradiated biocomposites showed the new formation of C1s (C–O–C) and O1s (O=C–O) peaks, probably a result of the slightly increased cross-linking reaction (C–O–C bonding type) and enhanced interfacial adhesion (esterification: O=C–O bonding type) between RHF and the matrix polymer compared with the nonirradiation samples. Based on the study results presented here, we recommend the use of low-dose EB irradiation as a suitable surface-treatment method to improve the interfacial interaction between matrix polymer and biofiller, as it offers several advantages such as not needing chemical reagents, and that it is a noncatalytic, environmentally friendly process which is easily automated.

*Acknowledgements:* This work was supported by the *Brain Korea 21 project*.

[1] M. Bengtsson, P. Gatenholm, K. Oksman, *Compos. Sci. Technol.* **2005**, *65*, 1468.
[2] H.-S. Kim, H.-S. Yang, H.-J. Kim, H.-J. Park, *J. Therm. Anal. Calorim.* **2004**, *76*, 395.
[3] H.-S. Yang, H.-J. Kim, H.-J. Park, B.-J. Lee, T.-S. Hwang, *Compos. Struct.* **2006**, *72*, 429.

 

[4] S. Mohanty, S. K. Verma, S. K. Nayak, *Compos. Sci. Technol.* **2006**, *66*, 538.
[5] G. Cantero, A. Arbelaiz, R. Llano-Ponte, I. Mondragon, *Compos. Sci. Technol.* **2003**, *63*, 1247.
[6] A. V. Gonzalez, J. M. Cervantes-Uc, R. Olayo, P. J. Herrera-Franco, *Compos., Part B* **1999**, *30*, 321.
[7] S. Mishra, A. K. Mohanty, L. T. Drzal, M. Misra, G. Hinrichsen, *Macromol. Mater. Eng.* **2004**, *289*, 955.
[8] X. Yuan, K. Jayaraman, D. Bhattacharyya, *Compos., Part A* **2004**, *35*, 1363.
[9] D. H. Han, S. H. Shin, S. Petrov, *Radiation Phys. Chem.* **2004**, *66*, 239.
[10] J. Raghavan, M.R. Baillie, *Polym. Compos.* **2000**, *21(4)*, 619.
[11] E. A. Abramyan, "*Industrial Electron Accelerators and Applications*", Hemisphere Publishing Co., New York 1998, pp. 1–30.
[12] B. Chen, K. Sun, *Polym. Test.* **2005**, *24*, 64.
[13] B. Zsigmond, L. Halasz, T. Czvikovszky, *Nucl. Instrum. Methods Phys. Res.* **2003**, *208*, 247.
[14] C. Albano, J. Reyes, M. Ichazo, J. Gonzalez, M. Brito, D. Moronta, *Polym. Degrad. Stab.* **2002**, *76*, 191.
[15] M. Pervaiz, M. M. Sain, *Macromol. Mater. Eng.* **2003**, *288*, 553.
[16] M. Modesti, A. Lorenzetti, D. Bon, S. Besco, *Polym. Degrad. Stab.* **2005**, *91*, 672.
[17] V. Hristov, S. Vasileva, *Macromol. Mater. Eng.* **2003**, *288*, 798.
[18] H. Kaczmarek, D. Oldak, P. Malanowski, H. Chaberska, *Polym. Degrad. Stab.* **2005**, *88*, 189.
[19] M. A. Khan, K. M. I. Ali, F. Yoshir, K. Makuuchi, *Angew. Makromol. Chem.* **1999**, *772*, 94.
[20] G. H. Yew, A. M. Mohd-Yusof, Z. A. M. Ishak, U. S. Ishiaku, *Polym. Degrad. Stab.* **2005**, *90*, 488.
[21] H.-S. Kim, H.-S. Yang, H-J. Kim, B.-J. Lee, T. S. Hwang, *J. Therm. Anal. Cal.* **2005**, *81*, 299.
[22] P. V. Joseph, K. Joseph, S. Thomas, C. K. S. Pillai, V. S. Prasad, G. Groeninckx, M. Sarkissova, *Compos., Part A* **2003**, *34*, 253.
[23] S. C. J. Loo, C. P. Ooi, Y. C. F. Boey, *Biomaterials* **2005**, *26*, 3809.
[24] T. Czvikovszky, *Radiat. Phys. Chem.* **2004**, *47*, 425. V. Tserki, P. Matzinos, S. Kokkou, C. Panayiotou, *Compos., Part A* **2005**, *36*, 965.
[25] V. Tserki, P. Matzinos, S. Kokkou, C. Panayiotou, *Compos., Part A* **2005**, *36*, 965.
[26] S. M. Lee, S. W. Choi, Y. C. Nho, H. H. Song, *J. Polym. Sci., Part B: Polym. Phys.* **2005**, *43*, 3019.
[27] S. Massey, D. Roy, A. Adnot, *Nucl. Instrum. Methods Phys. Res.* **2003**, *208*, 236.
[28] N. M. Stark, L. M. Matuana, *Polym. Degrad. Stab.* **2004**, *86*, 1.

 